DOI: http://dx.doi.org/10.26483/ijarcs.v16i3.7288

ISSN No. 0976-5697

Volume 16, No. 3, May-June 2025

International Journal of Advanced Research in Computer Science

RESEARCH PAPER

Available Online at www.ijarcs.info

THYROID MALIGNANCY DETECTION USING ARTIFICIAL INTELLIGENCE

Shiwangi Kulhari
Department of Physical Sciences,
Banasthali University, Tonk, India

Abhimanyu Singh Kulhari
Department of Computer Science,
Banasthali University, Tonk, India

Dr. Ritu Vijay
Department of Physical Sciences,
Banasthali University, Tonk, India

Abstract: The rise in thyroid cancer cases and the issue of unreliable false positive diagnostic rates in expert-reviewed ultrasound images underscore the need for precise tumor diagnosis. Convolutional Neural Networks (CNNs), a cutting-edge deep learning technique, offer remarkable capabilities in tackling computer vision challenges. This paper introduces a fine-tuned VGG-19 CNN model tailored to multi-classify thyroid nodules in pre-processed ultrasound (US) images. The experimental results demonstrate that the proposed model achieves accuracies of 0.6521, 0.7572, and 0.9201 for 50, 100, and 150 epochs, respectively. Notably, the optimal testing loss manifests at the 100-epoch juncture, signifying an equilibrium between effective model training and generalization. Moreover, an intriguing observation is the gradual enhancement in Grad-CAM visualizations with increasing epochs, indicating the model's evolving proficiency in discerning pertinent features associated with thyroid malignancy.

Keywords: thyroid cancer; convolutional neural networks; vgg-19 CNN model; fine-tuned; ultrasound (US) images

1. INTRODUCTION

Within the neck lies an essential endocrine gland recognized as the Thyroid gland, just in front of the trachea. It consists of two lobes, resembling the shape of wings, and is connected by an isthmus. During physical examination, thyroid is typically not palpable through the skin. This crucial gland plays a significant role in the body's hormonal regulation by utilizing iodine to produce hormones. These hormones are responsible for controlling essential bodily functions, including body temperature, heart rate, blood pressure, and the basal metabolic rate. The thyroid's proper functioning is essential for maintaining overall health and well-being [1] [2].

Thyroid cancer often manifests as an enlargement of the thyroid gland. Tumors that are well-differentiated and encapsulated can be palpable and may lead to voice changes and breathing difficulties [3].Thyroid cancer stands as the most prevalent form of endocrine malignancy, constituting approximately 2.1% of the total global cancer cases. The frequency of thyroid cancer occurrences has shown a consistent rise over recent decades in numerous countries [4]. Thyroid cancer ranks as the ninth most prevalent cancer type among males and the fifth most often cancer type among women [1][5].

Thyroid cancer has shown a significant increase in incidence since the late 1980s, surpassing the rise observed in any other form of cancer. Numerous research endeavors have indicated that the utilization of ultrasonography for screening purposes has played a crucial role in contributing to this upward trend. Thyroid malignancy is commonly linked with certain risk factors, for example female gender, family history of thyroid cancer, hormone therapy, history of benign thyroid diseases, high body mass index(BMI), exposure to radiation, tobacco use, environmental pollutants, alcohol consumption, and dietary factors [5][6]. Ultrasound (US) imaging serves as a extensively employed diagnostic method to identify and delineate characteristics of thyroid nodules. Nonetheless, evaluating whole-slide images is tedious as well as arduous for thyroid specialists [7]. Furthermore, approach has limitations due to the possibility of human error, leading to unreliable false-positive diagnostic rates [8].

Convolutional Neural Networks (CNNs) are a common form of deep learning methodology characterized by fully trainable models, and they are widely acknowledged as a cutting-edge technique in the field of image classification [9][10]. LeNet, AlexNet, NIN, ResNet, GoogLeNet, Xception and VGG represent a range of CNN models [11]. VGG (Visual Geometry Group)[12] is commonly used for classification tasks due to its architectural simplicity and effectiveness in learning complex features from images This study proposes a fine-tuned VGG-19 convolutional neural network model to multi-classify thyroid tumor. Additionally, it can empower doctors to make informed therapy decisions for their patients. In this paper, the contribution of this task along these lines is represented –

- The pre-trained VGG19 convolutional neural network model undergoes fine-tuning by modifying the filter quantities and strategically incorporating dropout layers with suitable parameters following the convolutional layers.
- The VGG19 model, which has been fine-tuned, is evaluated across three distinct epochs: 50, 100, and 150. The proposed model demonstrates enhancements in accuracy and significant decline in loss function value.

2. LITERATURE SURVEY

Zhu et al. have created a three-layer feed-forward artificial neural network (ANN) model with a 6-8-1 configuration [13]. Ma et al. have devised a model centred around cascade deep convolutional neural networks (CNNs), incorporating two distinct CNNs alongside an innovative splitting method. In the first CNN, ground-correct data were employed to establish a grasp of segmentation probability maps and the second CNN was used for the automated detection of thyroid tumors within sonographic thyroid images [14]. Liu et al have conducted a transfer of a CNN model trained on a substantial reference dataset to a novel ultrasound image dataset to address the challenge of limited sample size. Hybrid classification was employed on a hybrid feature space, formed by amalgamating traditional features with deep features [15]. Chi et al. have utilized feature extraction through fine-tuning the pre-trained Google Le Net model and then for classification random Forest classifier is fed with extracted features [16].

Li et al. have devised a hybrid model by combining ResNet-50 and Darknet-19 architectures [17]. Zhang et al. have introduced an innovative approach that involved the utilization of two integrated classification modules to effectively segregate thyroid nodules. [18]. Ko et al. have utilized pre-trained imagenet-vgg-f and pre-trained imagenet-vgg-verydeep16, in the recognition task after undergoing a fine-tuning process [19]. Moussa et al. have conducted fine-tuning of the resNet-50 model for thyroid malignancy detection [20]. Nguyen et al. have combined Res Net and Inception Net CNN models to enhance information extraction [21].

Liang et al. have classified thyroid and breast nodules through multi-organ Computer-Aided Diagnosis (CAD) system employing convolutional neural networks (CNNs) to classify thyroid and breast nodules. They explored the effects of various pre-processing approaches on diagnostic efficiency [22]. Wang et al. have conducted a comparative analysis between radiomics and deep learning-based technique i.e. fine-tuned VGG-16 for classifying thyroid nodules [23]. Xie et al. have introduced a unique structural design that combined local binary pattern with deep learning methodologies [24]. Liu et al. have devised an innovative joint convolutional neural network (CNN) that leverages information fusion techniques. This advanced CNN architecture comprises two distinct branched pathways, each dedicated to profound feature extraction [25]. Vadhiraj et al. have performed c a relative analysis between artificial neural network (ANN) classification algorithms and the support vector machine (SVM) [26]. Li et al. have created a holistic automated system for recognizing and classifying CT images of thyroid tumors. Their approach hinged on convolutional neural networks (CNNs) to drive the recognition and classification processes seamlessly [27].

Hang has presented a method that entails amalgamating conventional features with deep features to create a combined feature domain. A comparison between two models: ResNet18, a 18-layer residual convolutional neural network, and Res-GAN is done [28]. Peng et al. have created ThyNet model, which amalgamated ResNet, DenseNet, and ResNeXt architectures [29]. Qi et al. have developed a comprehensive network model named Mask-RCNN18. This model incorporated the feature pyramid network (FPN) and the residual network (ResNet) for feature extraction, employed the region proposal network (RPN) for classification, and integrated bounding box (BB) regression for generating Regions of Interest (ROI) to detect the existence of significant extrathyroidal extension (ETE) in cases of thyroid cancer.[30].Liu et al. have created a deep-learning model known as ThyNet-LNM, designed specifically for assessing Lymph Node Metastasis (LNM) [31]. Ajilisa et al. have integrated inception modules with squeeze and excitation networks to enhance the recognition accuracy of the inception network. Additionally, as a bridging dataset breast ultrasound images are used for multi-level transfer learning [32].

3. MATERIALS AND METHODS

This segment is structured into four main parts: dataset, data preprocessing, classical VGG-19 Model, and proposed fine-tuning strategy for the VGG-19 Model. The initial part outlines the collection and acquisition process of ultrasound images. The second part covers the image preprocessing steps. In the third part, the classical VGG-19 model is detailed. Lastly, the fourth section elucidates the strategy employed to fine-tune the VGG-19 model.

3.1. Dataset

In this study, a public open access dataset i.e. the Digital Database of Thyroid Ultrasound Images (DDTI) encompassing assessment of 347 B-mode thyroid ultrasound images is used. These images were derived from video sequences of thyroid ultrasounds captured using ultrasound devices, specifically TOSHIBA Nemio MX and TOSHIBA Nemio 30. Two experienced radiologists assessed these images in a group of 299 patients with thyroid-related conditions. Each image is paired with a detailed annotation and diagnostic description stored in an XML file. TIRADS (Thyroid Imaging Reporting and Data System) system is used by radiologists for classification of patients. TIRADS assigns points to different ultrasound features of a nodule, granting extra points to more suspicious features. The overall TI-RADS score is calculated by summing up the feature points across all categories, such as (TR1) normal thyroid, (TR2) benign, (TR3) absence of suspicious ultrasound features, (TR4a) presence of single suspicious ultrasound feature, (TR4b) 2 suspicious ultrasound features, (TR4c) 3 or 4 suspicious ultrasound features and (TR5) 5 suspicious ultrasound features. The XML files also contained the corresponding TI-RADS descriptions. In this dataset, the experts delineated the edges of the nodules and annotated distinct features such as veins, trachea, muscles, arteries, and calcifications. [33][34].

3.2. Data preprocessing

The images are cropped to specific dimensions, ensuring that the cropped region maintains a square shape. Subsequently, these images are converted to a single channel to ensure data consistency, reduce dimensionality, and enable gray scale-specific processing by transforming RGB images into grayscale. A sequence of additional image processing operations, including thresholding, denoising, contour detection, and resizing, generates processed images ready for subsequent analysis or utilization. The dataset is partitioned into training (consisting of 300 ultrasound images), validation (comprising 13 ultrasound images), and test (consisting of 34 ultrasound images) sets. This partitioning establishes the foundation for training, fine-tuning, and evaluating the proposed model. This data separation ensures the model's capacity to generalize effectively to previously unseen data.

3.3. Classical VGG-19 model

The VGG-19 architecture, initially presented by Simonyan and Zisserman [35] in 2014 is a deep convolutional neural network consisting of a total of 19 layers.. Its primary purpose is to categorize images into one thousand different object classes. To achieve this, the ImageNet database is used for VGG-19 training, which comprises 10 lakhs images across those one thousand categories. This architecture has gained significant popularity in classification of images tasks because of its effective utilization of numerous 3×3 filters within every convolutional layer. Figure 1 illustrates the VGG-19 architecture, which comprises 16 convolutional layers responsible for feature extraction, succeeded by three fully-connected layers dedicated to classification. The feature extraction layers are organized into 5 blocks, with each block being succeeded by a max-pooling layer. 224×224 dimensions image is a input to the model and the object's label present in the image is displayed in model's output [36].

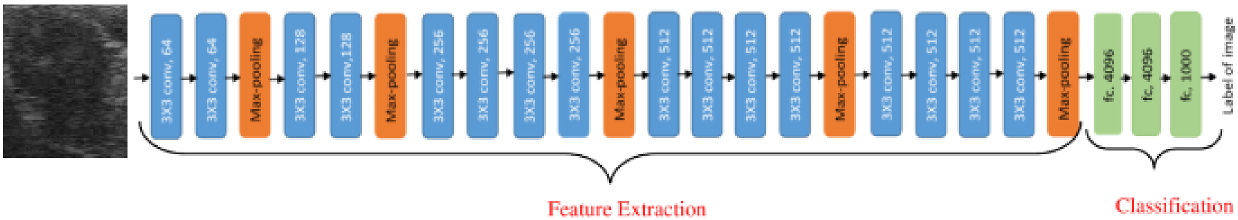

Fig.1. VGG-19 architecture [36]

3.4. Fine-tuning strategy for the VGG-19 Model

Fine-tuning of the CNN model involves adjusting the parameters of a pre-trained neural network to make it suitable for a specific task or dataset. Fine-tuning permits the model to utilize the learned features from the original dataset while adapting to the new task's characteristics. It also reduces training time by utilizing pre-trained weights as starting point. Employing pre-trained model is also beneficial in light of limited thyroid malignancy dataset, as pre-trained model brings general knowledge from its original training.

The proposed model incorporates 16 convolutional layers with ReLU activation, 5 max pooling layers and 2 fully-connected layers with ReLU activation and output fully-connected layer with softmax activation. The fine-tuning of pre-trained VGG-19 model incorporates 9 batch normalization layers, to normalize activations within mini-batches. It also introduces 11 dropout layers to strike a balance between fitting the training data well and generalizing effectively to new data. The pre-trained VGG-19 model is also modified by adjusting the number of filters. Filters in early layers typically capture basic features, while in deeper layers capture more complex features. Adjusting the filter parameters provides a way to control the trade-off between model complexity and computational efficiency. He Normal initialization method is used in convolutional layers to aid faster and more stable convergence during training by providing well-scaled initial weights that match well with the characteristics of ReLU activations. 0.0001 is the learning rate of model and adam optimizer is utilized for model's compilation. Employment of categorical cross-entropy loss function is done to classify thyroid nodules in 6 TIRADS categories with minimum loss and improved classification performance.

4. EXPERIMENTAL RESULTS

This segment provides a comprehensive analysis of the conducted experiments and their outcomes. It encompasses three key components, including the experimental setup, evaluation indexes, and the results and discussion.

4.1. Experimental Setup

The experiment was carried out on a computer equipped with an NVIDIA RTX A5000 graphics card featuring 24 gigabytes (GB) of GPU memory. The experimental setup employs a 64-bit Windows 10 operating system. The deep learning environment consists of Python 3.10 and Keras 2.3.1, utilizing TensorFlow GPU 1.16 as the backend. The model is trained for 50, 100 and epochs, encompassing distinct phases of learning and refinement

4.2. Evaluation Indexes

Accuracy is employed to assess the overall or average performance of a classification system. It refers to the closeness of measurement results to the true value. As presented in equation (1), it measures how well the system correctly classifies instances in relation to the total count of instances.

$$Accuracy = \frac{(TNC + TPC)}{(TNC + TPC + FNC + FPC)} \quad (1)$$

Where, TNC=True negative cases tally; TPC= True positive cases tally; FNC=False negative cases tally; FPC=False positive cases tally

A graph depicting the training and testing loss is employed to serve as a tool for evaluating performance by assessing how well the model fits the data. It helps to determine whether the model is overfitting, underfitting, or achieving a balanced fit. This graph displays the change in loss values over the course of training and testing iterations, offering insights into how well the model is learning and generalizing. Grad-CAM (Gradient-weighted Class Activation Mapping) is also used as performance indicator, which is a method to visualize the areas within an input image that hold the highest significance for a specific model's prediction. It highlights the regions that significantly contribute to the model's decision-making process.

4.3. Results and Discussion

A comparison of the accuracy of the fine-tuned VGG-19 model over 50, 100, and 150 epochs for thyroid malignancy detection is presented in table 1. As shown in the table, the accuracy of the proposed model increases with an increase in the number of training epochs. At 50 epochs, it achieves an accuracy of 0.6521, which improves to 0.7572 at 100 epochs, and further increases to 0.9201 at 150 epochs. The trend of increasing accuracy with more epochs indicates that the model's performance benefits from additional training. As the model receives more exposure to the training data, it refines its learned representations, fine-tunes its parameters, and becomes better at distinguishing between thyroid malignancy and non-malignancy cases.

Table1. Accuracy of VGG19 over 50,100 and 150 epochs

S.No.	Accuracy	Model Training (Epochs)
1	0.6521	**50**
2	0.7572	**100**
3	0.9201	**150**

Figure 2 displays the training and testing loss curves. Over 50 epochs of fine-tuned VGG19 training for thyroid malignancy detection, a noticeable gap emerged between the training and testing losses as shown in fig. 2.(b). The training loss, indicating optimization progress, decreased with learning. Conversely, the testing loss, evaluating unseen data, remained notably higher, hinting at potential overfitting. Extending training to 100 epochs lowered the testing loss compared to 50 epochs as illustrated in fig. 2. (c), while a slight uptick was seen at 150 epochs as presented in fig. 2. (d). The optimal loss value is thus inferred to be attained around 100 epochs for effective thyroid malignancy detection.

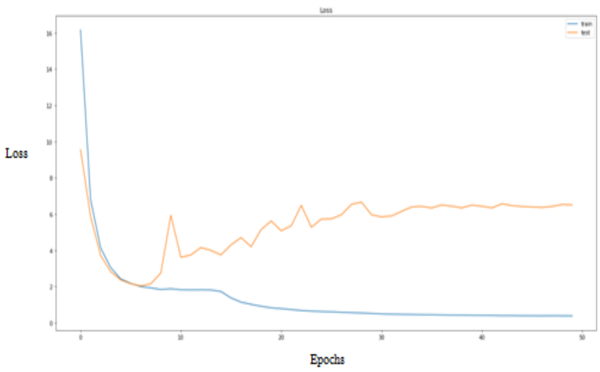

(a)

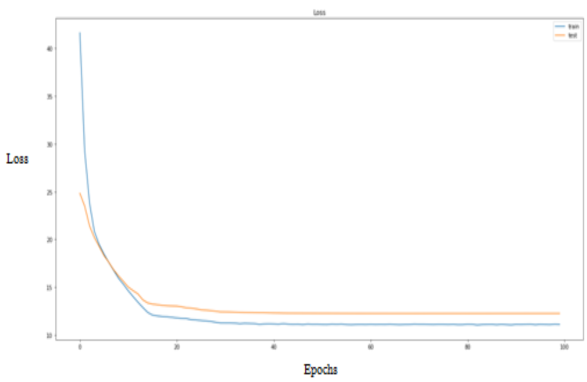

(b)

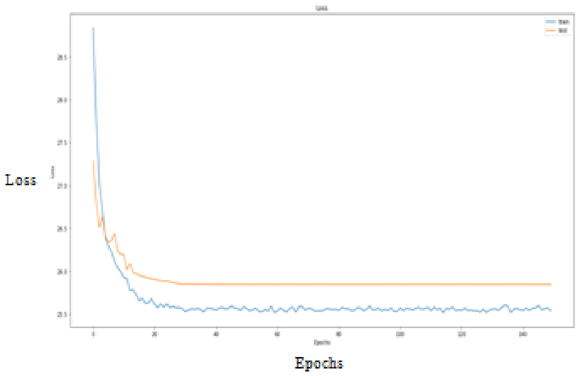

(c)

Fig.2. (a) Training and Testing loss at 50 Epochs (b) Training and Testing loss at 100 Epochs (c) Training and Testing loss at 150 Epochs

Figure 3 showcases Grad-CAM visualizations extracted from the trained model across 50, 100, and 150 epochs for thyroid malignancy detection. Notably, as the model is trained for progressively more epochs, the visualizations depict increasingly distinct and precise areas. This phenomenon signifies the model's growing ability to identify pertinent patterns and features linked to thyroid malignancy, leading to enhanced accuracy in its detections.

(a)

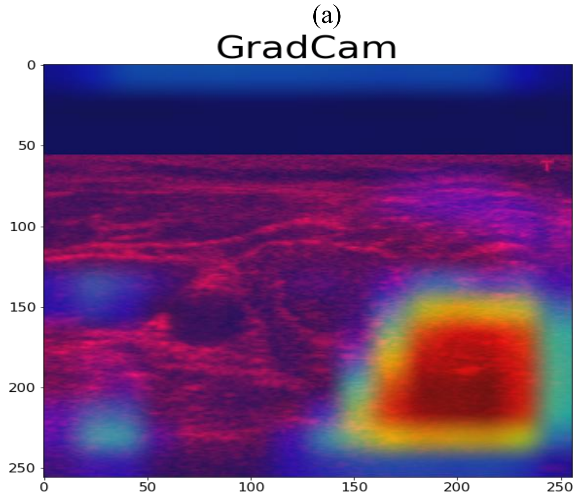

(b)

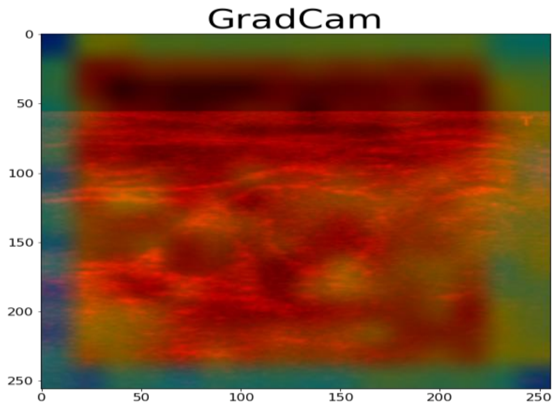

(C)

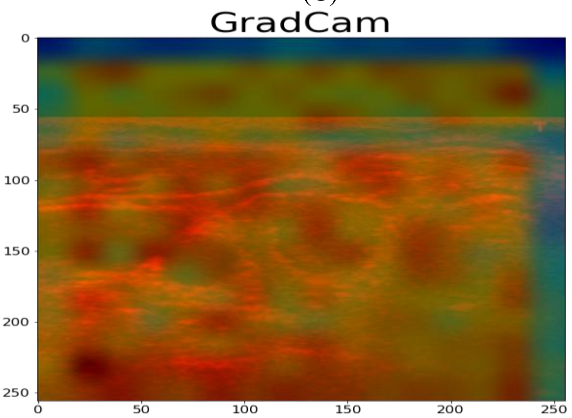

(d)

Fig.3. (a) Original image (b) Grad-CAM image for 50 Epochs (c) Grad-CAM image for 100 Epochs (d) Grad-CAM image for 150 Epochs

5. CONCLUSION

This paper introduced a fine-tuned VGG-19 model for multi-classification of thyroid nodules. By utilizing a pre-trained VGG-19 network, the model efficiently learns a new task without necessitating the creation and training of a new network. This approach not only accelerates the learning process through transfer learning but also addresses data scarcity concerns, ultimately saving training time. Furthermore, the experimental outcomes demonstrate a consistent enhancement in both accuracy and visualization of Gradient-weighted Class Activation Mapping (Grad-CAM) images as the number of epochs increases. Notably, the optimum testing loss is observed at the 100-epoch mark. This aligns with the model's capability to progressively refine its classification accuracy while producing more focused visualizations of relevant features.

REFERENCES

[1] Nguyen, Q. T., Lee, E. J., Huang, M. G., Park, Y. I., Khullar, A., & Plodkowski, R. A. (2015). Diagnosis and treatment of patients with thyroid cancer. American health & drug benefits, 8(1), 30–40.

[2] Cancer of the Thyroid - Cancer Stat Facts. (n.d.). SEER. https://seer.cancer.gov/statfacts/html/thyro.html

[3] Thyroid cancer - Symptoms and causes. (2023, April 26). Mayo Clinic. https://www.mayoclinic.org/diseases-conditions/thyroid-cancer/symptoms-causes/syc-20354161

[4] Kitahara, C. M., Körmendiné Farkas, D., Jørgensen, J. O. L., Cronin-Fenton, D., & Sørensen, H. T. (2018, March 23). Benign Thyroid Diseases and Risk of Thyroid Cancer: A Nationwide Cohort Study. The Journal of Clinical Endocrinology & Metabolism, 103(6), 2216–2224. https://doi.org/10.1210/jc.2017-02599

[5] Wang, Q., Huang, H., Zhao, N., Ni, X., Udelsman, R., & Zhang, Y. (2020, February 1). Phytoestrogens and Thyroid Cancer Risk: A Population-Based Case–Control Study in Connecticut. Cancer Epidemiology, Biomarkers & Prevention, 29(2), 500–508. https://doi.org/10.1158/1055-9965.epi-19-0456

[6] Drozd, V., Branovan, D. I., & Reiners, C. (2020, November 30). Increasing Incidence of Thyroid Carcinoma: Risk Factors and Seeking Approaches for Primary Prevention. International Journal of Thyroidology, 13(2), 95–110. https://doi.org/10.11106/ijt.2020.13.2.95

[7] Anari, S., Tataei Sarshar, N., Mahjoori, N., Dorosti, S., & Rezaie, A. (2022, August 25). Review of Deep Learning Approaches for Thyroid Cancer Diagnosis. Mathematical Problems in Engineering, 2022, 1–8. https://doi.org/10.1155/2022/5052435

[8] Zhang, X., Lee, V. C. S., Rong, J., Liu, F., & Kong, H. (2022). Multi-channel convolutional neural network architectures for thyroid cancer detection. PloS one, 17(1), e0262128. https://doi.org/10.1371/journal.pone.0262128

[9] Tajbakhsh, N., Shin, J. Y., Gurudu, S. R., Hurst, R. T., Kendall, C. B., Gotway, M. B., & Liang, J. (2016, May). Convolutional Neural Networks for Medical Image Analysis: Full Training or Fine Tuning? IEEE Transactions on Medical Imaging, 35(5), 1299–1312. https://doi.org/10.1109/tmi.2016.2535302

[10] Shin, H. C., Roth, H. R., Gao, M., Lu, L., Xu, Z., Nogues, I., Yao, J., Mollura, D., & Summers, R. M. (2016, May). Deep Convolutional Neural Networks for Computer-Aided Detection: CNN Architectures, Dataset Characteristics and Transfer Learning. IEEE Transactions on Medical Imaging, 35(5), 1285–1298. https://doi.org/10.1109/tmi.2016.2528162

[11] Zhang, Q., Zhang, M., Chen, T., Sun, Z., Ma, Y., & Yu, B. (2019, January). Recent advances in convolutional neural network acceleration. Neurocomputing, 323, 37–51. https://doi.org/10.1016/j.neucom.2018.09.038

[12] Simonyan, K., & Zisserman, A. (2014). Very deep convolutional networks for large-scale image recognition. arXiv preprint arXiv:1409.1556.

[13] Zhu, L. C., Ye, Y. L., Luo, W. H., Su, M., Wei, H. P., Zhang, X. B., Wei, J., & Zou, C. L. (2013, December 16). A Model to Discriminate Malignant from Benign Thyroid Nodules Using Artificial Neural Network. PLoS ONE, 8(12), e82211. https://doi.org/10.1371/journal.pone.0082211

[14] Ma, J., Wu, F., Jiang, T., Zhu, J., & Kong, D. (2017, April 17). Cascade convolutional neural networks for automatic detection of thyroid nodules in ultrasound images. Medical Physics, 44(5), 1678–1691. https://doi.org/10.1002/mp.12134

[15] Liu, T., Xie, S., Yu, J., Niu, L., & Sun, W. (2017, March). Classification of thyroid nodules in ultrasound images using deep model-based transfer learning and hybrid features. 2017 IEEE International Conference on Acoustics, Speech and Signal Processing (ICASSP). https://doi.org/10.1109/icassp.2017.7952290

[16] Chi, J., Walia, E., Babyn, P., Wang, J., Groot, G., & Eramian, M. (2017, July 10). Thyroid Nodule Classification in Ultrasound Images by Fine-Tuning Deep Convolutional Neural Network. Journal of Digital Imaging, 30(4), 477–486. https://doi.org/10.1007/s10278-017-9997-y

[17] Li, X., Zhang, S., Zhang, Q., Wei, X., Pan, Y., Zhao, J., Xin, X., Qin, C., Wang, X., Li, J., Yang, F., Zhao, Y., Yang, M., Wang, Q., Zheng, Z., Zheng, X., Yang, X., Whitlow, C. T., Gurcan, M. N., . . . Chen, K. (2019, February). Diagnosis of thyroid cancer using deep convolutional neural network models applied to sonographic images: a retrospective, multicohort, diagnostic study. The Lancet Oncology, 20(2), 193–201. https://doi.org/10.1016/s1470-2045(18)30762-9

[18] Zhang, H., Zhao, C., Guo, L., Li, X., Luo, Y., Lu, J., & Xu, H. (2019, October). Diagnosis of Thyroid Nodules in Ultrasound Images Using Two Combined Classification Modules. 2019

12th International Congress on Image and Signal Processing, BioMedical Engineering and Informatics (CISP-BMEI). https://doi.org/10.1109/cisp-bmei48845.2019.8965903

[19] Ko, S. Y., Lee, J. H., Yoon, J. H., Na, H., Hong, E., Han, K., Jung, I., Kim, E., Moon, H. J., Park, V. Y., Lee, E., & Kwak, J. Y. (2019, February 4). Deep convolutional neural network for the diagnosis of thyroid nodules on ultrasound. Head & Neck, 41(4), 885–891. https://doi.org/10.1002/hed.25415

[20] Moussa, O., Khachnaoui, H., Guetari, R., & Khlifa, N. (2019, August 16). Thyroid nodules classification and diagnosis in ultrasound images using fine-tuning deep convolutional neural network. International Journal of Imaging Systems and Technology, 30(1), 185–195. https://doi.org/10.1002/ima.22363

[21] Nguyen, D. T., Kang, J. K., Pham, T. D., Batchuluun, G., & Park, K. R. (2020, March 25). Ultrasound Image-Based Diagnosis of Malignant Thyroid Nodule Using Artificial Intelligence. Sensors, 20(7), 1822. https://doi.org/10.3390/s20071822

[22] Liang, X., Yu, J., Liao, J., & Chen, Z. (2020, January 10). Convolutional Neural Network for Breast and Thyroid Nodules Diagnosis in Ultrasound Imaging. BioMed Research International, 2020, 1–9. https://doi.org/10.1155/2020/1763803

[23] Wang, Y., Yue, W., Li, X., Liu, S., Guo, L., Xu, H., Zhang, H., & Yang, G. (2020). Comparison Study of Radiomics and Deep Learning-Based Methods for Thyroid Nodules Classification Using Ultrasound Images. IEEE Access, 8, 52010–52017. https://doi.org/10.1109/access.2020.2980290

[24] Xie, J., Guo, L., Zhao, C., Li, X., Luo, Y., & Jianwei, L. (2020, December 1). A Hybrid Deep Learning and Handcrafted Features based Approach for Thyroid Nodule Classification in Ultrasound Images. Journal of Physics: Conference Series, 1693(1), 012160. https://doi.org/10.1088/1742-6596/1693/1/012160

[25] Liu, Z., Zhong, S., Liu, Q., Xie, C., Dai, Y., Peng, C., Chen, X., & Zou, R. (2021, January 6). Thyroid nodule recognition using a joint convolutional neural network with information fusion of ultrasound images and radiofrequency data. European Radiology, 31(7), 5001–5011. https://doi.org/10.1007/s00330-020-07585-z

[26] Vadhiraj, V. V., Simpkin, A., O'Connell, J., Singh Ospina, N., Maraka, S., & O'Keeffe, D. T. (2021, May 24). Ultrasound Image Classification of Thyroid Nodules Using Machine Learning Techniques. Medicina, 57(6), 527. https://doi.org/10.3390/medicina57060527

[27] Li, W., Cheng, S., Qian, K., Yue, K., & Liu, H. (2021, May 27). Automatic Recognition and Classification System of Thyroid Nodules in CT Images Based on CNN . Computational Intelligence and Neuroscience, 2021, 1–11. https://doi.org/10.1155/2021/5540186

[28] Hang, Y. (2021, July 22). Thyroid Nodule Classification in Ultrasound Images by Fusion of Conventional Features and Res-GAN Deep Features. Journal of Healthcare Engineering, 2021, 1–7. https://doi.org/10.1155/2021/9917538

[29] Peng, S., Liu, Y., Lv, W., Liu, L., Zhou, Q., Yang, H., Ren, J., Liu, G., Wang, X., Zhang, X., Du, Q., Nie, F., Huang, G., Guo, Y., Li, J., Liang, J., Hu, H., Xiao, H., Liu, Z., . . . Xiao, H. (2021, April). Deep learning-based artificial intelligence model to assist thyroid nodule diagnosis and management: a multicentre diagnostic study. The Lancet Digital Health, 3(4), e250–e259. https://doi.org/10.1016/s2589-7500(21)00041-8

[30] Qi, Q., Huang, X., Zhang, Y., Cai, S., Liu, Z., Qiu, T., Cui, Z., Zhou, A., Yuan, X., Zhu, W., Min, X., Wu, Y., Wang, W., Zhang, C., & Xu, P. (2023, April). Ultrasound image-based deep learning to assist in diagnosing gross extrathyroidal extension thyroid cancer: a retrospective multicenter study. EClinicalMedicine, 60, 102007. https://doi.org/10.1016/j.eclinm.2023.102007

[31] [31] Liu, Y., Lai, F., Lin, B., Gu, Y., Chen, L., Chen, G., Xiao, H., Luo, S., Pang, Y., Xiong, D., Li, B., Peng, S., Lv, W., Alexander, E. K., & Xiao, H. (2023, June). Deep learning to predict cervical lymph node metastasis from intraoperative frozen section of tumour in papillary thyroid carcinoma: a multicentre diagnostic study. EClinicalMedicine, 60, 102007. https://doi.org/10.1016/j.eclinm.2023.102007

[32] Ajilisa, O. A., Jagathy Raj, V. P., & Sabu, M. K. (2023, July 24). A Deep Learning Framework for the Characterization of Thyroid Nodules from Ultrasound Images Using Improved Inception Network and Multi-Level Transfer Learning. Diagnostics, 13(14), 2463. https://doi.org/10.3390/diagnostics13142463

[33] Pedraza, L., Vargas, C., Narváez, F., Durán, O., Muñoz, E., & Romero, E. (2015, January 28). An open access thyroid ultrasound image database. SPIE Proceedings. https://doi.org/10.1117/12.2073532

[34] Song, R., Zhang, L., Zhu, C., Liu, J., Yang, J., & Zhang, T. (2020). Thyroid Nodule Ultrasound Image Classification Through Hybrid Feature Cropping Network. IEEE Access, 8, 64064–64074. https://doi.org/10.1109/access.2020.2982767

[35] Simonyan, K., & Zisserman, A. (2014, September 4). Very Deep Convolutional Networks for Large-Scale Image Recognition. arXiv.org. https://arxiv.org/abs/1409.1556v6

[36] Bansal, M., Kumar, M., Sachdeva, M., & Mittal, A. (2021, September 17). Transfer learning for image classification using VGG19: Caltech-101 image data set. Journal of Ambient Intelligence and Humanized Computing, 14(4), 3609–3620. https://doi.org/10.1007/s12652-021-03488-z

